

---

# Synthesis of New Chalcogenides from the System $\text{GeTe}_6\text{-Cu}$ and a Layered Structure Based on Them and an Azo Polymer for Application in the Optoelectronic

---

[Yordanka Trifonova](#)\*, [Ani Stoilova](#), [Deyan Dimov](#), [Georgi Mateev](#), [Dimana Nazarova](#), [Lian Nedelchev](#), [Vladislava Ivanova](#), [Vanya Lilova](#)

Posted Date: 10 July 2025

doi: 10.20944/preprints202507.0904.v1

Keywords: transition metal doped chalcogenides; azo polymers; Ge-Te-Cu



Preprints.org is a free multidisciplinary platform providing preprint service that is dedicated to making early versions of research outputs permanently available and citable. Preprints posted at Preprints.org appear in Web of Science, Crossref, Google Scholar, Scilit, Europe PMC.

Copyright: This open access article is published under a Creative Commons CC BY 4.0 license, which permit the free download, distribution, and reuse, provided that the author and preprint are cited in any reuse.

Disclaimer/Publisher's Note: The statements, opinions, and data contained in all publications are solely those of the individual author(s) and contributor(s) and not of MDPI and/or the editor(s). MDPI and/or the editor(s) disclaim responsibility for any injury to people or property resulting from any ideas, methods, instructions, or products referred to in the content.

Article

# Synthesis of New Chalcogenides from the System GeTe<sub>6</sub>-Cu and a Layered Structure Based on Them and an Azo Polymer for Application in the Optoelectronic

Y. Trifonova <sup>1,\*</sup>, A. Stoilova <sup>1,2</sup>, D. Dimov <sup>1,2</sup>, G. Mateev <sup>1,2</sup>, D. Nazarova <sup>1,2</sup>, L. Nedelchev <sup>1,2</sup>, V. Ivanova <sup>1</sup> and V. Lilova <sup>1</sup>

<sup>1</sup> University of Chemical Technology and Metallurgy, Department of Physics, 8 Kl. Ohridski Blvd., 1756 Sofia, Bulgaria

<sup>2</sup> Institute of Optical Materials and Technologies – Bulgarian Academy of Sciences, Acad. Georgi Bonchev Bl.109, 1113 Sofia, Bulgaria

\* Correspondence: danche@uctm.edu

## Abstract

New bulk chalcogenides from the system (GeTe<sub>6</sub>)<sub>1-x</sub>Cu<sub>x</sub>, where x=5, 10, 15 и 20 mol %, has been synthesized. The structure and composition of the materials was studied using X-ray powder diffraction (XRD) and energy dispersive spectroscopy (EDS). Scanning electron microscopy (SEM) has been applied to analyze the surface morphology of the samples. Some thermal characteristics as glass transition, crystallization and melting temperature and some physicochemical properties as density, compactness, molar and free volume were also determined. The XRD pattern shows sharp diffraction peaks indicating that the synthesized new bulk materials are crystalline. The following four crystal phases were determined: Te, Cu, CuTe и Cu<sub>2</sub>GeTe<sub>3</sub>. The results from the EDS confirm the presence of Ge, Te and Cu in the bulk samples in a concentration in good correspondence with those theoretically determined. A layered thin film material based on the synthesized new Ge<sub>4</sub>Te<sub>5</sub>Cu<sub>5</sub> chalcogenide, which has the most flexible structure, and the azo polymer PAZO has been fabricated, and the kinetic of the photoinduced birefringence at 444 nm has been measured. The results indicate an increase in the maximal induced birefringence for the layered structure in comparison to the non-doped azo polymer film.

**Keywords:** transition metal doped chalcogenides; azo polymers; Ge-Te-Cu

## 1. Introduction

Among the chalcogen family, tellurium-based are of special interest as they demonstrate industrial valuable phase transition by being heated through an electrical current [1] or upon irradiation with light [2], which has already been used in rewriteable optical discs [3] and electronic 3D memory chips [4]. Since the commercialization of the GeSbTe [5] and of the AgInSbTe [6] as information storage media, many investigations have been carried out in order to improve the optical and electrical contrasts between the crystalline and glassy phase, to increase the number of reversible phase transitions, etc. A lot of them involve synthesis of Ge-Sb-Te or quaternary alloy (Ag, In)-doped Sb<sub>2</sub>Te with different concentrations of constituent elements [7,8], adding of dopants [9], introduction of Se and/or S into the matrix [10], incorporation of another chemical element in place of Sb [11,12]. Regarding the latter, it was reported by Y. Sutou et al that the crystallization starting time of an amorphous GeCu<sub>2</sub>Te<sub>3</sub> film is as fast as that of an amorphous GeSbTe film, but it can be re-amorphized by laser irradiation at lower power and shorter pulse [13]. Dongol et al synthesized Ge-Te-Cu bulk glassies with higher thermal stability compared to the Ge-Sb-Te system [14]. Furthermore, it was

found that Cu–Ge–Te alloys exhibit smaller density change upon crystallization and the crystalline phase has a lower optical reflectivity than the amorphous one [15,16]. The observed results have been attributed to the copper d-electrons giving rise to different nature of the bonding between the structural units in amorphous and crystalline phase compared to the p-bonded chalcogenides [17]. Since, Ge-Te based chalcogenides doped with transition-metal have gathered attention as previously overlooked and underexplored materials for optoelectronic application. Many other interesting properties has also been reported for the Ge-Te-Cu system including resistance to oxidation, relatively high electrical conductivity, low heat conductivity, high Seebeck coefficient, high transmittance, low absorbance, and reflectance in the visible/near-infrared region, but high absorbance in the ultraviolet region [18]. In last years, a significant scientific effort has also been paid on the development of composite or hybrid materials combining the advantages of the chalcogenides with those of other materials [19–21]. An attractive class among them represent the azo dyes or polymers with embedded chalcogenide particles or prepared as multilayer structures, where the optical recording capability of the azo chromophores has been significantly enhanced after incorporation of the nanoparticles into the polymer matrix or as result of interface effects between the stacked films [22,23].

In the present article we report on the synthesis of new chalcogenides from the system Ge-Te-Cu, their structural investigation and determination of some physico-chemical properties. Furthermore, a layer-by-layer structure based on one of the synthesized new chalcogenides and the azo polymer PAZO has been fabricated, and the kinetic of photo-induced birefringence has been studied. The idea for this investigation originates from previously reported by a part from our research group increase in the maximum induced birefringence in PAZO polymer based composite materials dopped with various nanoparticles [24–26]. In all these studies, the composite thin film materials were fabricated through spin coating of dispersion containing the azo polymer and the nanoparticles. In the case of chalcogenides as dopant [27], this technology has shown many challenges related to proper grinding of the synthesized as bulk material chalcogenides or their insolubility in aqueous media and methanol, in which the PAZO is good soluble. Tellurium-rich chalcogenides are well known for their high tendency to crystallize, especially in bulk form, but also prepared as thin film. A replicated crystalline surface structure of the underlying chalcogenide film in the top layer of the PAZO polymer may play role similar to that of the embedded nanoparticles. To the best of our knowledge, no results from measuring the photoinduced birefringence in a bilayer structure of a chalcogenide and an azo polymer has been reported up to day.

## 2. Materials and Methods

### 2.1. Synthesis of the New Chalcogenides from the Ge-Te-Cu System and Preparation of the Bilayer Structure

The bulk samples from the system  $(\text{GeTe}_6)_{1-x}\text{Cu}_x$ , where  $x=5, 10, 15$  и  $20$  mol %, were synthesized by conventional melt quenching technique. High-purity Ge, Te and Cu, respectively Ge and Te – 5N and Cu – 4N, were weighed in appropriate mol % proportions, put into quartz ampoule and sealed in vacuum under residual pressure of  $1.33 \cdot 10^{-3}$  Pa. The ampoules were then placed in a muffle furnace (Firemagic FM4 Plus), heated at a rate of  $5 \cdot 10^2$  K/s to a final temperature of  $1373^\circ\text{C}$  and kept at this temperature for 2 h. During the heating process, the ampoules were frequently shaken for better homogenization of the melt constituent. Afterward, the samples were quenched in ice-water mixture at cooling rate of  $1 \cdot 10^2$  K/s. Finally, the bulk samples were taken from the quartz tube and cut into slices.

The azo polymer poly[1-4-(3-carboxy-4-hydrophenylazo) benzensulfonamido]-1,2-ethanediyl, sodium salt], denoted as PAZO throughout the text below, was purchased from Sigma Aldrich (Prod. #346411).

For the preparation of the non-doped PAZO polymer film, 44.6 mg from the PAZO polymer were dissolved in 1200  $\mu\text{l}$  methanol by means of a magnetic stirrer (IKA  $\text{\textcircled{R}}$  RET B 8000). The mixture was stirred for one hour at 1700 rpm by room temperature. A drop of 130  $\mu\text{l}$  from the resulting

solution was deposited on a quartz substrate and spin coated for 60 seconds at 1000 rpm. The substrate was cleaned and polished in advance.

For the preparation of the layered structure, the bulk chalcogenide was evaporated from a quartz evaporator on a quartz substrate using the vacuum-thermal evaporation technique. The layer was deposited at evaporation rate of 1 Å/s. The pressure was kept below  $2.10^{-6}$  mbar. The thickness and the deposition rate were controlled by a QCM-quartz crystal microbalance (INFICON SQM-160), which together with the substrate holder was placed 12 cm above the evaporator. The azo polymer film was deposited onto the chalcogenide film by spin-coating a drop of 130  $\mu$ l from the solution prepared for the fabrication of the non-doped PAZO polymer film for 60 seconds at 1000 rpm.

## 2.2. Methods Used for Characterization of the Synthesized New Chalcogenides and Measuring the Kinetic of the Photoinduced Birefringence

The XRD experiment were carried out at "Philips" powder diffractometer working in the Bragg-Brentano ( $\theta$ - $2\theta$ ) geometry, with a  $\text{CuK}\alpha$  radiation ( $\lambda = 1,54060.10^{-10}\text{m}$ ) and a graphite monochromator for the reflected beams. The XRD patterns were obtained for 75 s at constant scan rate and reflection angle of  $2\theta$  in the scan range from  $15^\circ$  to  $70^\circ$  with a scan step of  $0.05^\circ$ .

Scanning electron microscope (EVO MA 10 „Carl Zeiss“) connected with EDX (Energy Dispersive X-ray detector system „Bruker“) was used to study the surface morphology (at 10 000x and 30 000 magnification) and chemical composition of the synthesized new bulk chalcogenides. The micrograph of the  $\text{Ge}_{14}\text{Te}_{81}\text{Cu}_5$  film was obtained using scanning electron microscope Philips 515 with acceleration voltage of 30 kV and magnification 10 000x.

Differential scanning calorimetry (NETZSCH DSC 404 F3) was used to determine the glass transition, crystallization and melting temperature of the new chalcogenides. The DSC analysis was carried out by heating 11 mg of each sample in fine powdered form at a constant heating rate of 10 K/min, and the change in heat flow with reference to an empty aluminum pan were measured.

The thicknesses of the films were determined by a high precision profilometer "Talystep" with an accuracy of  $\pm 5$  nm. The measured thickness of the pure PAZO polymer film was 300 nm, of the chalcogenide film 30 nm and of the spin coated PAZO polymer onto the chalcogenide layer 292 nm.

The density of the bulk samples was estimated by pycnometer technique, with an accuracy of  $\pm 0.7\%$ , using water as immersion fluid. The compactness of the materials was calculated according the equation given below:

$$\delta = \frac{\sum_i \frac{c_i A_i}{\rho_i} - \sum_i \frac{c_i A_i}{\rho}}{\sum_i \frac{c_i A_i}{\rho}} \quad (1)$$

where  $\rho$  is the density of the sample,  $\rho_i$ ,  $A_i$  and  $c_i$  are the density, the atomic mass and the  $i$ -th component atomic fraction, respectively.

The molar volume,  $V_m$ , was calculated using equation (2):

$$V_m = \frac{1}{\rho} \sum_i c_i A_i \quad (2)$$

The free volume percentage, FVP, was obtained in accordance with equation (3):

$$\text{FVP} = \frac{V_m - V_T}{V_m} \cdot 100, \% \quad (3)$$

where  $V_T$  is the theoretical molar volume determined as a sum of the molar volumes of the components multiplied by the atomic fraction of each of them (equation 4).

$$V_T = \sum_{i=1}^n c_i V_i \quad (4)$$

## 2.3. Optical Setup for Measuring the Photo-Induced Birefringence

A classical polarimetric setup [28] was used to induce birefringence ( $\Delta n$ ) at wavelength of 444 nm of the pump laser beam (Coherent cube, intensity 330 mW/cm<sup>2</sup>) in a film spot area of approximately 0,2 cm<sup>2</sup>. The writing laser was vertically polarized. A linearly polarized at  $45^\circ$  beam from a diode-pumped solid-state (DPSS) laser, with wavelength 635 nm was used as a probe beam. The parameters of Stokes of the output beam were measured by a PAX5710 Polarization Analyzing

System (Thorlabs). The value of the induced birefringence was then calculated according equation (5).

$$\Delta n = \frac{\lambda}{2\pi d} \arctan\left(\frac{S_3}{S_2}\right) \quad (5)$$

where  $\lambda$  is the wavelength of the probe laser,  $d$  is the film thickness, and  $S_2$  and  $S_3$  are two of the four components of the Stokes vector.

### 3. Results

The XRD pattern shows sharp diffraction peaks indicating that the synthesized bulk chalcogenide materials are crystalline (Figure 1). The following four crystal phases were determined: hexagonal Te (JCPDS card № 36-1452), cubic Cu (JCPDS card № 85-1326), orthorhombic CuTe (JCPDS card № 07-0110) and orthorhombic Cu<sub>2</sub>GeTe<sub>3</sub> [29]. Based on the data obtained, it can be assumed that the synthesized new chalcogenides consist of GeTe<sub>4</sub> and CuTe<sub>4</sub> tetrahedra and tellurium chains.

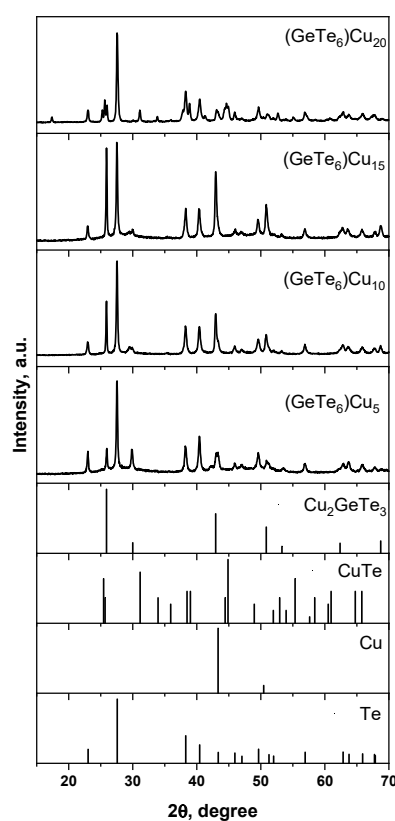
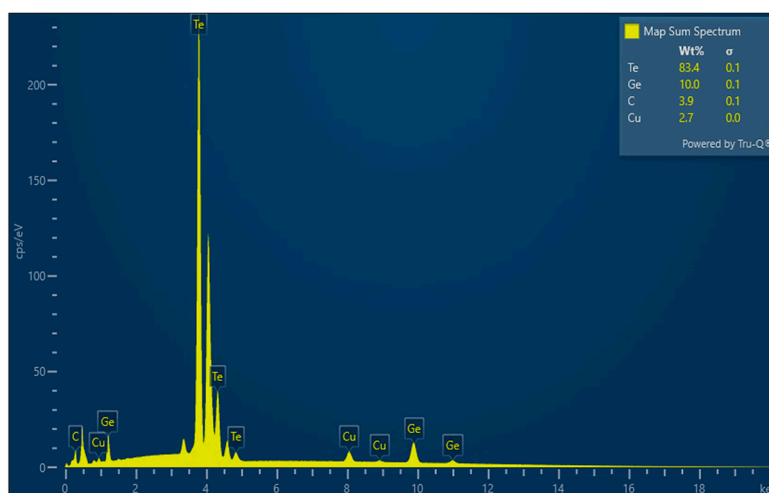


Figure 1. XRD patterns of the samples from the system GeTe<sub>6</sub>-Cu.

Figure 2 presents the energy-dispersive spectrum obtained for the sample containing 5 mol% Cu, which indicates the presence of germanium, copper and tellurium in the material studied. Peaks corresponding to these chemical elements has also been observed in the spectra of the samples containing 10, 15 and 20 mol % Cu.



**Figure 2.** Energy-dispersive spectrum of sample  $\text{Ge}_{14}\text{Te}_{81}\text{Cu}_5$ .

Table 1 summarizes the data obtained from the EDS analysis concerning the amount of Ge, Cu and Te present in the samples studied. For comparison, it is given the theoretically determined amount of Ge, Cu and Te for each of the synthesized composition. The results from the EDS confirm the presence of Ge, Te and Cu in the bulk samples in a concentration in good correspondence with those theoretically determined.

**Table 1.** EDS elemental analysis (expressed in percentage of weight) and comparison with the calculated elemental concentration in mol % converted to weight percent (wt. %).

Sample mol %	Theoretically determined elemental concentration, wt. %	Elemental concentration determined by EDS, wt. %
$\text{Ge}_{14}\text{Te}_{81}\text{Cu}_5$	Ge – 8.7	Ge – $10.0 \pm 0.1$
	Te – 88.6	Te – $83.4 \pm 0.1$
	Cu – 2.7	Cu – $2.7 \pm 0.0$
$\text{Ge}_{13}\text{Te}_{77}\text{Cu}_{10}$	Ge – 8.3	Ge – $6.6 \pm 0.1$
	Te – 86.1	Te – $82.2 \pm 0.1$
	Cu – 5.6	Cu – $5.6 \pm 0.0$
$\text{Ge}_{12}\text{Te}_{73}\text{Cu}_{15}$	Ge – 7.8	Ge – $7.9 \pm 0.1$
	Te – 83.6	Te – $76.5 \pm 0.1$
	Cu – 8.6	Cu – $9.7 \pm 0.0$
$\text{Ge}_{11}\text{Te}_{69}\text{Cu}_{20}$	Ge – 7.3	Ge – $0.7 \pm 0.0$
	Te – 81.0	Te – $71.3 \pm 0.1$
	Cu – 11.7	Cu – $9.2 \pm 0.0$

On Figure 3 are presented SEM images revealing the morphology of the synthesized new bulk materials and of the  $\text{Ge}_{14}\text{Te}_{81}\text{Cu}_5$  film. The electron micrographs of the bulk sample containing 5 mol % Cu shows the presence of single, different in shape and size, white crystals, which could be attributed to the  $\text{GeTe}_4$  and  $\text{CuTe}_4$  tetrahedral structural units. With increasing the Cu amount in the samples, the crystals become more and larger. For the sample doped with 20 mol. % Cu, some of the crystals have a rectangular parallelepiped-like shape with a length between 1.0 and 2.2  $\mu\text{m}$  and a height between 1.4 and 2.6  $\mu\text{m}$ . Other form clusters of smaller or larger crystals. On all the images, long tellurium chains with metallic luster are observed. The micrograph from the surface of the  $\text{Ge}_{14}\text{Te}_{81}\text{Cu}_5$  film shows the presence of a lot of well-defined grains. They are almost uniformly distributed into the Te and Cu matrix and have parallelepiped-like form with a length and height of about 90-140 nm. According to the obtained XRD data, the bulk  $\text{Ge}_{14}\text{Te}_{81}\text{Cu}_5$  sample consists of tellurium, which is in higher amount in comparison to the other components, and of approximately

equal amounts of Cu and  $\text{Cu}_2\text{GeTe}_3$ , the latter consisting of  $\text{GeTe}_4$  and  $\text{CuTe}_4$  tetrahedra forming an orthorhombic crystal lattice. Therefore, the observed grains could be contributed to the  $\text{Cu}_2\text{GeTe}_3$  phase.

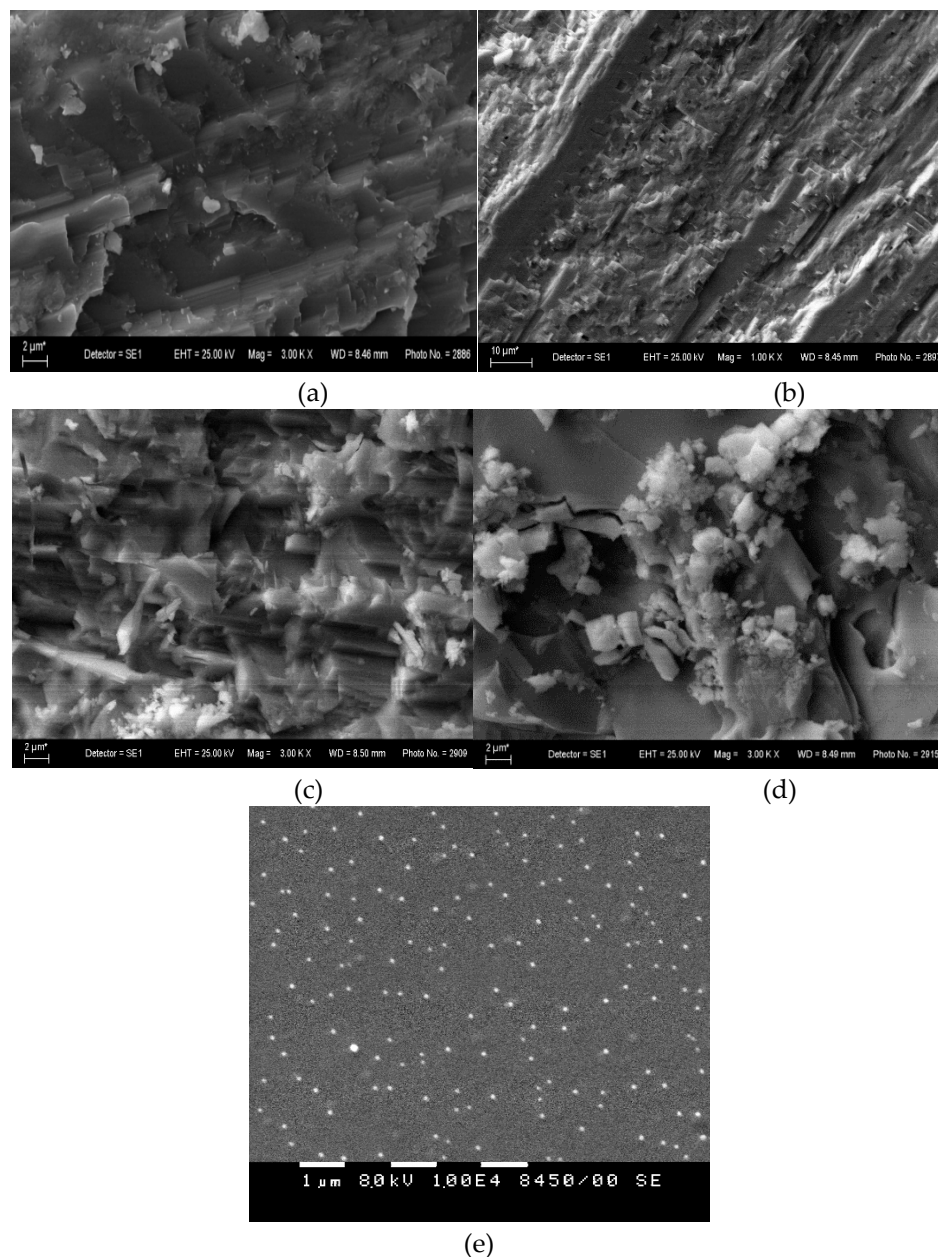


**Figure 4.** SEM images of the bulk samples studied (a, b, c and d) and of the  $\text{Ge}_{14}\text{Te}_{81}\text{Cu}_5$  film (e).

Figure 5 presents the results from the carried-out thermal analysis. The DSC curve for sample  $\text{Ge}_{14}\text{Te}_{81}\text{Cu}_5$  shows glass transition temperature ( $T_g$ ) at  $139^\circ\text{C}$ . With increasing the Cu content,  $T_g$  decreases and takes a value of  $T_g = 121^\circ\text{C}$  for  $\text{Ge}_{13}\text{Te}_{77}\text{Cu}_{10}$  and  $T_g=114^\circ\text{C}$  for  $\text{Ge}_{12}\text{Te}_{73}\text{Cu}_{15}$  and  $\text{Ge}_{11}\text{Te}_{69}\text{Cu}_{20}$ . The thermogram of the sample containing 5 mol % Cu shows an exothermic peak at  $229^\circ\text{C}$ , which corresponds to the crystallization temperature ( $T_c$ ) of the material. For the sample doped with 10 mol % Cu,  $T_c = 206^\circ\text{C}$  as the observed exothermic peak is more clearly expressed compared to this one obtained for sample  $\text{Ge}_{14}\text{Te}_{81}\text{Cu}_5$ . On the thermogram for samples  $\text{Ge}_{12}\text{Te}_{73}\text{Cu}_{15}$  and  $\text{Ge}_{11}\text{Te}_{69}\text{Cu}_{20}$  such peak is not to observed. The DSC curve for sample  $\text{Ge}_{14}\text{Te}_{81}\text{Cu}_5$  shows a clearly expressed endothermic peak corresponding to melting temperature ( $T_m$ ) at  $369^\circ\text{C}$ . The shoulder at  $387^\circ\text{C}$  indicates the presence of two crystalline phases, the first one being in higher concentration. Based on the obtained XRD data, it could be assumed that the peak at  $369^\circ\text{C}$  corresponds to tellurium and the shoulder at  $387^\circ\text{C}$  to  $\text{Cu}_2\text{GeTe}_3$  crystalline phase. The DSC curves for the samples containing 10 mol % and 15 mol % Cu show a double melting peak, with two clearly expressed

maxima, respectively at 369°C and 381°C for  $\text{Ge}_{13}\text{Te}_{77}\text{Cu}_{10}$ , and at 369°C and 377°C for  $\text{Ge}_{12}\text{Te}_{73}\text{Cu}_{15}$ , which could be associated with the presence of tellurium and  $\text{Cu}_2\text{GeTe}_3$  crystalline phases in the material. The thermogram of sample  $\text{Ge}_{11}\text{Te}_{69}\text{Cu}_{20}$  shows an endothermic peak corresponding to melting temperature at 344°C and a shoulder at 363°C indicating the presence of two crystalline phases. Based on the obtained XRD data, we assume that these phases are Te and CuTe.

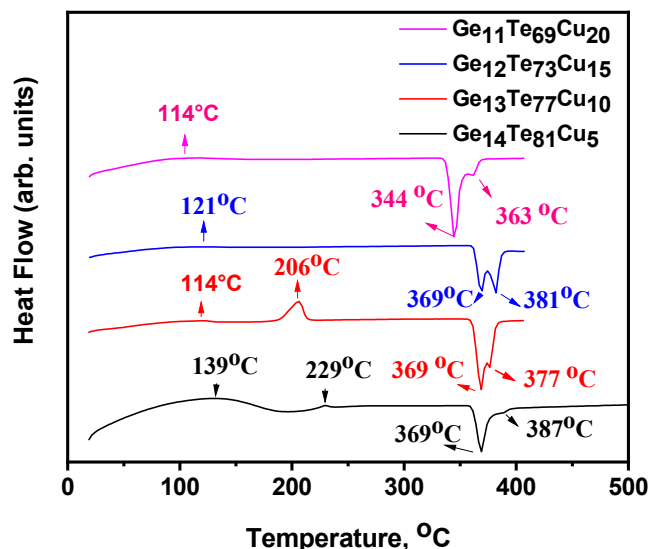


Figure 5. DSC curves of the samples studied.

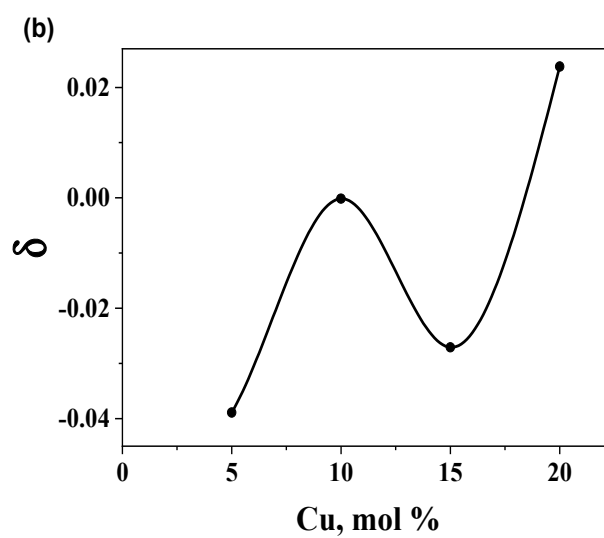
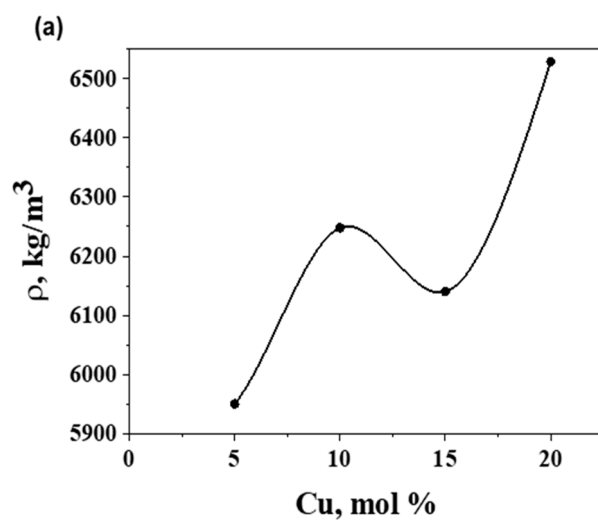
In Table 2 are presented the obtained values for the density, compactness, molar volume and free volume percentage of all the samples studied, and their dependence on the copper concentration are shown on Figure 6. As seen, the value of the density increases as the copper content increases. Since the size of the Ge and Cu atoms is close (atomic radii of 1.22 and 1.28 Å respectively), the observed increase in the density is probably due to the lowering in the tellurium content as the tellurium atom possess bigger atomic radii of 1.40 Å. The introduction of smaller atoms leads to formation of more dense structure as confirmed by other studies [30]. The dependence of the compactness on the copper concentration follows the same trend as the density, an increase with increasing the Cu content is observed. The increase in the concentration of atoms smaller in atomic radius and less heavy in weight (the atomic weight of Ge, Te and Cu is respectively 72.6 g.mol<sup>-1</sup>, 127.7 g.mol<sup>-1</sup> and 63.5 g.mol<sup>-1</sup>) leads to the formation of more compact and dense packaged structure. Figure 6c presents the molar volume of the materials as a function of the composition, and it is seen that  $V_m$  decreases with the addition of Cu. The observed reduction in the values can be viewed as defined by the following two facts: decrease in the molecular weight and increase in the density of the material. From Figure 6d it is seen, that the free volume percentage has a lowest value for the sample containing 20 mol% copper and highest value for the sample doped with 5 mol% Cu.

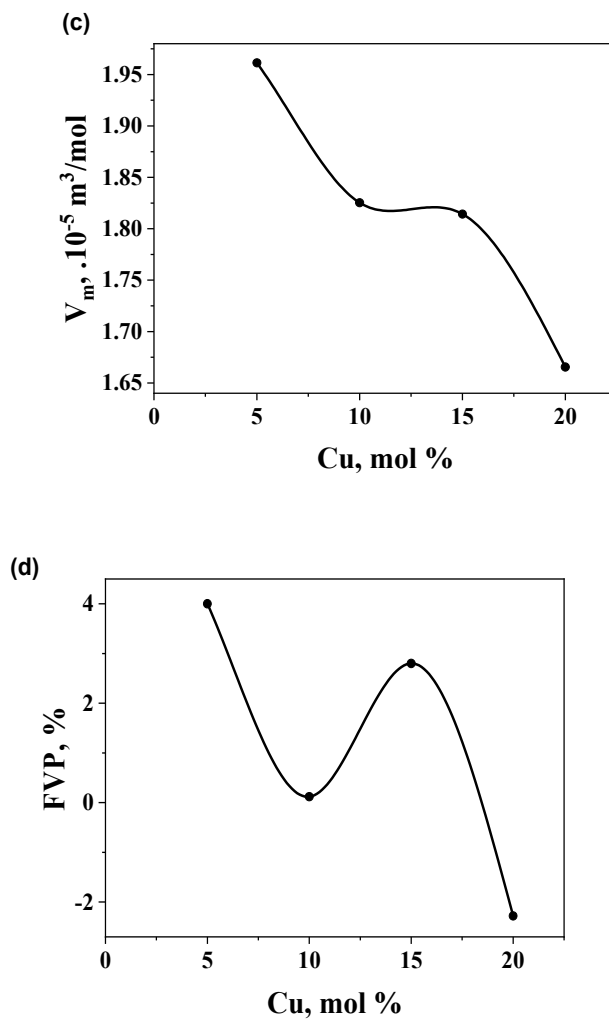
The functional relation between the studied physico-chemical features and the copper content shows similar trend of the curves, namely they increase or decrease with increasing the Cu concentration but not linearly. At around 10 mol % copper content there is a change in the slope of the curve. As explained by many authors [30], this non-linearity is probably due to structural transformation associated with tight bonding, shorter bond length and followed by sharp decrease of the volume.

Table 2. Physico-chemical properties of the bulk samples studied.

Sample	Density, 10 <sup>3</sup> kg/m <sup>3</sup>	Compactness, 10 <sup>-2</sup>	Molar volume, 10 <sup>-5</sup> m <sup>3</sup> /mol	FVP, %
$\text{Ge}_{14}\text{Te}_{81}\text{Cu}_5$	5.950	-3.890	1.961	4.00

$\text{Ge}_{13}\text{Te}_7\text{Cu}_{10}$	6.248	-0.015	1.825	0.12
$\text{Ge}_{12}\text{Te}_7\text{Cu}_{15}$	6.140	-2.709	1.814	2.80
$\text{Ge}_{11}\text{Te}_6\text{Cu}_{20}$	6.529	2.378	1.666	-2.28





**Figure 6.** Density (a), compactness (b), molar volume (c) and FVP (d) dependence on the composition.

In Figure 7 (a) are presented the results from measuring the kinetics of birefringence induced in the samples studied at 444 nm recording wavelength of the pump laser.

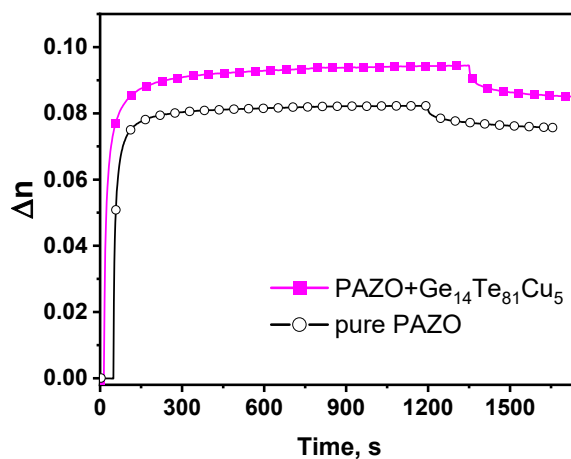


**Figure 7.** Birefringence kinetics for the samples studied induced at 444 nm.

For the pure PAZO polymer film, the maximal induced birefringence has a value of  $\Delta n_{\max} = 0.083$ . For the layer-by-layer structure an increase in the maximal induced birefringence, respectively  $\Delta n_{\max} = 0.095$ , has been measured.

#### 4. Discussion

Generally, the observed higher value of the  $\Delta n_{\max}$  for the bilayer structure based on the azo polymer and  $\text{Ge}_{14}\text{Te}_{81}\text{Cu}_5$  in comparison to the pure PAZO film could be viewed as result from: changes in the free volume and/or increased number of scattering and reflectance points within the top layer due to the underlying film morphology (i); interference effects between light reflected at the boundaries between the two layers (ii) and/or some photoinduced phenomena appear in the chalcogenide film contributing to the value of the measured birefringence (iii). Considering (i), a polymer layer spin-coated onto a chalcogenide film closely replicates the surface texture of the underlying film [31,32]. As shown on Figure 4e, there are a lot of grains on the surface of the chalcogenide film, which “copied” into the structure of the azo polymer layer increase the path length of the light within the film and provide opportunity for interaction of the photons with the azo chromophores at various angles. In such case, the  $\text{Ge}_{14}\text{Te}_{81}\text{Cu}_5$  film plays a role similar to that of the nano-particles used as dopant in PAZO polymer based composite materials, which according the main reported up to date hypothesis consists in increasing the free volume around the azo chromophores making the number of molecules capable for isomerization higher or in increasing the scattering inside the composite allowing excitation and reorientation of originally off-plane chromophores that would otherwise not contribute to the birefringence [33]. Considering (ii), when light interacts with a layer-by-layer structure, reflections or scatterings from the interface between the two layers can undergo constructive interference resulting in increased light intensity and since in enhanced birefringence of the top layer. Furthermore, scattering and reflectance effects may alter the polarization state of the incident light. These changes can lead to activation of azo chromophores, even those that are not inherently sensitive to the polarization of the incident light. Considering (iii), the photo-induced phenomena in chalcogenide materials upon irradiation with linearly polarized light are numerous, with different mechanism [34,35]. They are generally stronger in amorphous chalcogenides due to the more space for atomic movement (higher free volume) than in crystalline ones [36] and depend heavily on sufficient light intensity. By the studied bilayer structure, when the light enters the top layer, its intensity dramatically decreases before reaching the chalcogenide layer below as a result from the strong absorption of the azo chromophores at the used wavelength of the laser beam. Since the SEM image of the  $\text{Ge}_{14}\text{Te}_{81}\text{Cu}_5$  film suggests, even if is not confirmed, some polycrystallinity, and valuable photoinduced phenomena in chalcogenides require sufficient light intensity to occur, we believe on this stage of our investigation, that the observed higher value of the  $\Delta n_{\max}$  for the bilayer structure in comparison to the pure PAZO film is more due to (i) or (ii). These assumptions are under consideration in our ongoing investigations.

#### 5. Conclusions

New chalcogenides from the system  $(\text{GeTe}_6)_{1-x}\text{Cu}_x$ , where  $x=5, 10, 15$  и  $20$  mol %, has successfully been synthesized by one-step melt quenching technique. The obtained bulk materials consist of  $\text{GeTe}_4$  and  $\text{CuTe}_4$  tetrahedral structural units and Te-Te chains. With increasing the copper content, the glass transition temperature decreases from  $139^\circ\text{C}$  to  $114^\circ\text{C}$  as the crystallization temperature follows the same trend. The carried-out DSC analysis indicate also the presence of two crystalline phases in the bulk materials doped with 5, 10 and 15 mol% Cu, namely Te и  $\text{Cu}_2\text{GeTe}_3$ , and the presence of Te и CuTe crystal phases in the sample doped with 20 mol% Cu. The study of some physicochemical features of the new chalcogenides has shown the existence of a local extremum at 10 and 15 mol% Cu in the functional dependence of the density, compactness, molar volume and free volume on the copper concentration. The most flexible structure possesses sample  $\text{Ge}_{14}\text{Te}_{81}\text{Cu}_5$ . A layered thin film

material based on the synthesized new  $\text{Ge}_{14}\text{Te}_{81}\text{Cu}_5$  chalcogenide and the azo polymer PAZO has been fabricated, and the kinetic of the photoinduced birefringence at 444 nm has been measured. The results indicate an increase in the maximal induced birefringence for the layered structure ( $\Delta n_{\text{max}}=0.095$ ) in comparison to the non-doped azo polymer film ( $\Delta n_{\text{max}}=0.083$ ).

**Author Contributions:** Conceptualization, Y.T.; D.D and A.S.; methodology, Y.T.; D.D. and A.S.; validation, D.N. and L.N.; investigation, Y.T.; D.D.; V.L. and G.M.; data curation, Y.T.; D.D.; V.V. and G.M.; writing—original draft preparation, A.S. and Y.T.; writing—review and editing, D.N.; L.N.; Y.T.; supervision, D.N.; L.N.

**Funding:** This research was funded by the European Union-NextGeneration EU, through the National Recovery and Resilience Plan of the Republic of Bulgaria, project № BG-RRP-2.004-0002, "BiOrgaMCT".

**Data Availability Statement:** All data generated or analyzed during this study are included in the published article.

**Acknowledgments:** The authors gratefully acknowledge the support provided by the European Union-NextGeneration EU, through the National Recovery and Resilience Plan of the Republic of Bulgaria, project № BG-RRP-2.004-0002, "BiOrgaMCT". Research equipment of Distributed Research Infrastructure INFRAMAT, part of Bulgarian National Roadmap for Research Infrastructures, supported by Bulgarian Ministry of Education and Science was used in this investigation. G. Mateev and D. Nazarova are grateful for the funding from the Bulgarian National Science Fund (BNSF) through project KII-06-H88/2.

**Conflicts of Interest:** The authors declare no conflict of interest. The funders had no role in the design of the study; in the collection, analyses, or interpretation of data; in the writing of the manuscript; or in the decision to publish the results.

## References

1. Zhao, Z.; Clima, S.; Garbin, D.; Degraeve, R.; Pourtois, G.; Song, Z.; Zhu, M. Chalcogenide Ovonic Threshold Switching Selector. *Nanomicro Lett.* 2024, 11, pp. 16-81.
2. Ohta, T.; Ovshinsky, S. R.; Phase-Change Optical Storage Media. *Photo-Induced Metastability in Amorphous Semiconductors*; Kolobov A.V.; 1st ed.; Wiley-VCH, Weinheim, Germany, 2003; pp. 310-326.
3. Wuttig, M.; Yamada, N. Erratum: Phase-change materials for rewriteable data storage. *Nat. Mater.* 2007, 6, pp.1004–1004.
4. Fazio, A. Advanced technology and systems of cross point memory. *International Electron Devices Meeting (IEDM)*, San Francisco, CA, USA, 2020, 24.1.1–24.1.4.
5. Yamada, N.; Ohno, E.; Akahira, N.; Nishiuchi, K.; Nagata, K.; Takao, M. High Speed Overwritable Phase Change Optical Disk Material, *Jpn. J. Appl. Phys.* 1987, 26 61, pp. 61-66.
6. Iwasaki, H.; Harigaya, M.; Nonoyama, O.; Kageyama, Y.; Takahashi, M.; Yamada, K.; Deguchi, H.; Ide, Y. Completely Erasable Phase Change Optical Disc II: Application of Ag-In-Sb-Te Mixed-Phase System for Rewritable Compact Disc Compatible with CD-Velocity and Double CD-Velocity. *Jpn. J. Appl. Phys.* 1993, 32, 5241.
7. Fattorini, A. D.; Chèze, C.; García, I. L.; Petrucci, C.; Bertelli, M.; Riva, F. R.; Prili S.; Privitera S. M. S.; Buscema M.; Sciuto, A.; Franco, S.; D'Arrigo G.; Longo, M.; Simone, S.; Mussi, V.; Placidi, E.; Cyrille, M-C.; Tran, N-P.; Calarco, R.; Arciprete, F. Growth, electronic and electrical characterization of Ge-rich Ge–Sb–Te alloy. *Nanomater.* 2022, 13.
8. Petroni, E.; Allegra, M.; Baldo, M.; Laurin, L.; Andrea, S.; Favennec, L.; Desvoivres, L.; Sandrini, J.; Boccaccio, C.; Le-Friec, Y.; Ostrovsky, A.; Gouraud, P.; Bonneville, A.; Ranica, R.; Redaelli, A. Study of Ge-Rich Ge–Sb–Te device-dependent segregation for industrial grade embedded phase-change memory. *PSS RRL*, 2024, 18.
9. Zhou, X.; Zhou X.; Xia M.; Rao F.; Wu L.; Li X.; Song Z.; Feng S.; Sun H. Understanding phase-change behaviors of carbon-doped  $\text{Ge}_2\text{Sb}_2\text{Te}_5$  for phase-change memory application. *Appl. Mater. Interfaces* 2014, 6, pp. 14207–14214.

10. Golovchak, R.; Plummer, J.; Kovalskiy, A.; Holovchak, Y.; Ignatova, T.; Trofe, A.; Mahlovanyi, B.; Cebulski, J.; Krzeminski, P.; Shpotyuk, Y.; Boussard-Pledel, C.; Bureau B. Phase-change materials based on amorphous equichalcogenides. *Sci Rep* 2023, 13.
11. Malhotra, L. K.; Sripathi, Y.; Reddy G. B. Material science aspects of phase change optical recording. *Bull. Mater. Sci.*, 1995, 18, pp. 725-739.
12. Wang, G.; Shen, X.; Nie, Q.; Chen, F.; Wang, X.; Fu, J.; Chen, Y.; Xu, T.; Dai, S.; Zhang, W.; Wang, R. Te-based chalcogenide films with high thermal stability for phase change memory. *J. Appl. Phys.* 2012, 111, 093514-1- 093514-5.
13. Saito, Y.; Koike, J. Optical contrast and laser-induced phase transition in GeCu<sub>2</sub>Te<sub>3</sub> thin film. *Appl. Phys. Lett.* 2013, 102.
14. Dongol, M.; AbouZied, M.; Gamal, G.A.; El-Denglawey, A. Synthesis and the RDF fine structure of Ge<sub>0.15</sub>Te<sub>0.78</sub>Cu<sub>0.07</sub> bulk alloy. *Optik*, 2016, 127, pp. 8186-8193.
15. Skelton, J. M.; Kobayashi, K.; Sutou, Y.; Elliott, S. R. Origin of the unusual reflectance and density contrasts in the phase-change material Cu<sub>2</sub>GeTe<sub>3</sub>. *Appl. Phys. Lett.* 2013, 102, 224105.
16. Saito, Y.; Sutou, Y.; Koike, J. Phase change characteristics in GeTe-CuTe pseudobinary alloy films. *J. Phys. Chem. C* 2014, 118, pp. 26973–26980.
17. Saito, Y.; Sutou, Y.; Fons, P.; Shindo, S.; Kozina, X.; Skelton, J. M.; Kolobov, A.V.; Kobayashi, K.; Electronic Structure of Transition-Metal Based Cu<sub>2</sub>GeTe<sub>3</sub> Phase Change Material: Revealing the Key Role of Cu d Electrons. *Chem. Mater.* 2017, 29, pp. 7440–7449.
18. W. Ming; Chen L.; The microstructure and electrical and optical properties of Ge–Cu–Te phase-change thin films. *Cryst Eng Comm*, 2024, 26, pp. 395-405.
19. Mishra, S. P.; Krishnamoorthy, K.; Sahoo, R.; Kumar, A. Organic–inorganic hybrid polymers containing 3,4-ethylenedioxythiophene and chalcogens in the main chain. *J. Mater. Chem.* 2006, 16, pp. 3297-3304.
20. Gerbreder, A.; Teteris, J.; Kolobjonoks, V. Holographic recording in polymer composites of organic photochromes and chalcogenides, Sixth International Conference on Advanced Optical Materials and Devices, Riga, Latvia, 12.11.2008, 7142.
21. Bertelli, M.; Sfuncia, G.; De Simone, S.; Fattorini, A. D.; Calvi, S.; Mussi, V.; Arciprete, F.; Mio, A. M.; Calarco R.; Longo M. Stable chalcogenide Ge–Sb–Te heterostructures with minimal Ge segregation. *Sci Rep*, 2024, 14, 15713.
22. Berberova-Buhova, N.; Nedelchev, L.; Stoykova, E.; Nazarova D. Optical response evaluation of azopolymer thin solid films doped with gold nanoparticles with different sizes. *J. Chem. Technol. Metall*, 2022, 57, pp. 671-675.
23. Teteris J.; Gertners U. Optical field-induced surface relief formation on chalcogenide and azo-benzene polymer films, International Conference on Functional Materials and Nanotechnologies, Riga, Latvia, 17–20 April 2012.
24. Nazarova, D.; Nedelchev, L.; Sharlandjev, P.; Dragostinova, V. Anisotropic hybrid organic/inorganic (azopolymer/SiO<sub>2</sub> NP) materials with enhanced photoinduced birefringence. *Appl. Opt.* 2013, 52, E28–E33.
25. Mateev, G.; Nazarova, D.; Nedelchev, L. Increase of the Photoinduced Birefringence in Azopolymer Films Doped with TiO<sub>2</sub> Nanoparticles. *J. Phys. Technol.* 2019, 3, 18–21.
26. Nazarova, D.; Nedelchev, L.; Stoykova, E.; Blagoeva, B.; Mateev, G.; Karashanova, D.; Georgieva, B.; Kostadinova, D. Photoinduced birefringence in azopolymer doped with Au nanoparticles. *J. Phys. Conf. Ser.* 2019, 1310, 012018.
27. Stoilova, A.; Dimov, D.; Trifonova, Y.; Lilova, V.; Blagoeva, B.; Nazarova, D.; Nedelchev, L. Preparation, structural investigation and optical properties determination of composite films based on PAZO polymer doped with GeTe<sub>4</sub>-Cu chalcogenide particles. *Eur. Phys. J. Appl. Phys.* 2021, 95, 30301.
28. Nikolova, L.; Ramanujam, P.S. *Polarization Holography*; Cambridge University Press: Cambridge, UK, 2009.
29. Delgado G.; Mora, A.; Pirela, M. Velásquez-Velásquez, A.; Villarreal, M.; Fernández, B. Structural refinement of the ternary chalcogenide compound Cu<sub>2</sub>GeTe<sub>3</sub> by X-ray powder diffraction. *Phys. Stat. Sol. (a)*, 2004, 201, 2900.

30. Petkov, P.; Ilchev, P.; Ilcheva, V.; Petkova T.; Physico-chemical properties of Ge-Te-Ga glasses. *J. Optoelectron. Adv. M.* 2007, 9, pp. 3093 – 3096.
31. Tyona, M. D. A comprehensive study of spin coating as a thin film deposition technique and spin coating equipment, *Adv. Mater. Res.* 2013, 2, pp. 181-193.
32. Jemelka, J.; Palka, K.; Janicek, P.; Slang, S.; Jancalek, J.; Kurka M.; Vlcek M. Solution processed multi-layered thin films of Ge<sub>20</sub>Sb<sub>5</sub>S<sub>75</sub> and Ge<sub>20</sub>Sb<sub>5</sub>Se<sub>75</sub> chalcogenide glasses. *Sci Rep*, 2023, 13, pp. 16609.
33. Nazarova, D.; Nedelchev, L.; Berberova-Buhova, N.; Mateev G. Nanocomposite photoanisotropic materials for applications in polarization holography and photonics. *Nanomaterials*, 2023, 13, pp. 2946.
34. Krecmer, P.; Moulin, A. M.; Stephenson, R. J.; Rayment, T.; Welland, M. E.; Elliott S. R. Reversible Nanocontraction and Dilatation in a Solid Induced by Polarized Light. *Sci.* 1997, 277, pp. 1799-1802.
35. Tanaka, Ke.; Gotoh, T.; Nakayama, H. Anisotropic patterns formed in Ag–As–S ion-conducting amorphous semiconductor films by polarized light. *Appl. Phys. Lett.* 1999, 75, pp. 2256–2258.
36. Popescu, M. Disordered chalcogenide optoelectronic. *J. Optoelectron. Adv. M.* 2005, 7, pp. 2189 – 2210.

**Disclaimer/Publisher's Note:** The statements, opinions and data contained in all publications are solely those of the individual author(s) and contributor(s) and not of MDPI and/or the editor(s). MDPI and/or the editor(s) disclaim responsibility for any injury to people or property resulting from any ideas, methods, instructions or products referred to in the content.